Minimizing Distress on Flexible Pavements Using Variable Tire Pressure

By Philip M. O. Owende,[1] Anton M. Hartman,[2] Shane M. Ward,[3] Michael D. Gilchrist,[4] and Michael J. O'Mahony[5]

(Reviewed by the Air Transport Division)

Abstract: The potential of variable tire pressure technology to minimize distress on flexible pavements with thin asphalt surfacing layers and peat soil subgrade was evaluated using in-situ stress-strain data. Pavement interfacial strains and corresponding subgrade stresses imposed by a three-axle truck were measured and used to estimate the fatigue life of the surfacing layer. Three levels of truck wheel loads in combination with four tire inflation pressures (350, 490, 630, and 770 kPa) were used to evaluate the potential distress by the single steering wheel and rear dual wheels in tandem. Results suggest that lateral strain due to the single steering wheel is the most critical to fatigue failure, which is influenced by the viscoelastic nature of asphalt, and therefore truck speed and axle configuration are important. Lower tire pressures increased the fatigue life of the surfacing layer with respect to the rear dual wheels and the steering wheel by up to 200 and 300%, respectively. Haulage trucks with systems for managing variable tire pressure such as the central tire inflation systems may therefore enhance the serviceability of pavements overlying peat or other soft soil foundations.

INTRODUCTION

Background

Over one-third (190,000 ha) of the existing forest area in Ireland is on peatlands. These forests are accessed by basic road infrastructure (flexible pavements) predominantly laid on weak peat soil foundations. The peat-based roads deform easily under mechanical loading due to vehicular traffic, which accelerates their deterioration and imposes high repair and maintenance costs (O'Mahony et al. 2000). Transportation is therefore a costly factor in the overall timber production process, because of the necessity for reduced axle loads and smaller transportation vehicles with lower haulage rates [National Council for Forest Research Development (COFORD) 1994]. It accounts for up to 25% of the delivered cost of timber [Irish Forestry Board (Coillte) 1991].

It is well documented that reducing truck axle load decreases its road damaging potential exponentially (Lay 1990). Nevertheless, the economics of timber transportation necessitates a maximization of truck payload; hence, they must be loaded close to the legal limit (gross vehicle weight of 40 t or axle load limit of 10 t). However, the forestry industry recognizes the importance of achieving cost-effective timber haulage with minimum negative impact on the environment, and it identifies a need for the development and adoption of environmentally sensitive systems within the current Sustainable Forest Management program (Coillte 1998). Consequently, there are initiatives for improved management of the related road networks to enhance their serviceability and to

minimize the overall cost of their maintenance. Options that are being considered are (1) the improvement of design standards for new roads including the up-grading of weaker links in the present secondary road networks; and (2) the use of specialized trucks with variable tire pressure (VTP) systems.

VTP technology has been used successfully to moderate the impact of timber transportation trucks on unsurfaced roads (Foltz and Elliot 1997) and those susceptible to the periodic structural weakening condition of "spring-thaw" (Mahoney et al. 1994; Bradley 1996). However, its effectiveness on thin flexible pavements with peat or other soft soil substrata has not been investigated.

This project evaluates the potential of VTP to enhance the structural performance of forest access roads with thin asphalt surfacing layers and peat soil subgrade. Structural performance in this context refers to the fatigue cracking and surface rutting associated with trafficking by timber haulage vehicles.

VTP

Truck-tire inflation pressures are specified to permit the vehicles to carry a full payload at highway speeds with good handling and without overheating the tires (Dunlop 1998). Consequently, when a truck is empty, partially loaded or traveling at reduced speeds, the tires are overinflated for the respective operating conditions (Bradley 1993). Higher tire pressures contribute to the structural deformation of flexible pavements, which is manifested as functional or structural distress (i.e., defects on the surface or substratum, which determine serviceability). An additional benefit of a truck operating with low tire pressure (using VTP) is reduced vehicle vibration on low quality roads, which may result in lower truck maintenance costs.

VTP has significant benefits on paved and unpaved roads and in off-road operational conditions. On paved roads, structural strains are less if the tire pressure is adapted to the speed and tire loads (Grau 1993). Low tire pressure reduces the severity of cracking, which leads to an increased life expectancy of thin pavements. Computer modeling of such pavements has predicted that for a specified level of potential damage, lower tire pressure may allow about 10% reduction in the thickness of standard base course aggregate layer (Bradley 1997). Vehicle ride-comfort and shock loading are also improved due to the attenuation of mechanical vibrations (Tire 1998). On the other hand, a higher inflation pressure reduces tire deflections,

and consequently the tire stress, which increases the service life of the tire. Rolling resistance of the wheels is also reduced with possible savings in fuel consumption. However, at higher inflation pressures, there is greater variation in the tire-pavement contact stresses across the tire breadth, which is thought to cause differential wear on tires (De Beer et al. 1997).

On unpaved roads, low tire pressure causes less damage by rutting, rainfall runoff flow paths are shortened, and less sediment is therefore generated from the road surface (Foltz and Elliot 1997; Moore 1997). Reductions in sediment yield of up to 84% have been recorded for roads used by heavy haulage vehicles (Foltz 1994); this has major implications for the maintenance of high water quality standards to protect aquatic habitats in the forest environments. With respect to road design and construction, a reduction in aggregate surfacing thickness of 25–30% of the standard profile dimensions is possible when the haulage trucks employ VTP technology (Bradley 1997). To minimize road damage in regions that are susceptible to the road structure-weakening phenomenon of spring-thaw, restrictions are generally applied for heavy haulage vehicles such as timber trucks, with negative economic impacts. Operation of haulage trucks with low tire pressure provides an alternative to such load restrictions (Bradley 1996; Kestler et al. 1997) for extended haulage seasons. Traction capability of the haulage vehicles is also improved, therefore enhancing the productivity of the transportation system (shorter cycle times) under difficult forest road conditions.

In off-road applications such as the movement of machinery on the forest floor, soil compaction increases with tire inflation pressure (Jakobsen and Dexter 1989; Schwanghart 1991) due to the higher contact pressure at the tire-soil interface. For constant drawbar pull, slip is less at lower inflation pressures, and therefore soil damage is reduced. Other positive benefits of reduced inflation pressure include minimized wheel rutting (Raper et al. 1995), reduced rolling resistance and therefore improved fuel economy, and improved net traction and tractive efficiency (Burt and Bailey 1982).

Central Tire Inflation (CTI) is a system for managing VTP. It enables on-the-move tire pressure changes in response to changing terrain conditions. CTI systems generally comprise five component assemblies, namely, an air-compressor unit (auxiliary utility or brake system compressor), air control valves, air lines, rotary union hardware for transmit air into and out of rotating wheels, and a computerized control interface/panel for selection of appropriate tire pressures with respect to payload and speed of travel. If the air brake compressor system is used, air priority valves are included to protect the brake system's integrity, by allowing for tire inflation only when brake pressure is above a safe level. The truck speed is set relative to the tire pressure and load, to prevent damage, and there is an override if design speed limit warnings are ignored.

CTI was developed in the 1940s to improve the mobility of military vehicles on weak, poor traction surfaces such as desert sands (Bradley 1993). More recently, it has been adopted in the operation of timber haulage vehicles, due to its potential to reduce road damage and haulage costs associated with unsurfaced and poor quality forest access roads. It offers a readily accessible variable in vehicle operation that may be used to improve both vehicle performance and the impact of dynamic loads on the different terrain that are transversed by vehicles fitted with pneumatic tires; hence, it provides an environmentally sensitive strategy for heavy vehicle locomotion.

ANALYSIS OF FATIGUE DAMAGE OF FLEXIBLE PAVEMENTS

A flexible pavement is a multilayer structure composed of an asphalt surfacing layer and the combined unbound aggregate roadbase, on a subgrade of natural soil. Under service conditions, the stress state may be idealized as depicted in Fig. 1. Moving wheel loads cause the top and bottom of the pavement to shift rapidly from compression to tension, and fatigue cracks arise from the repeated tensile strains. According to elastic layer theory, the maximum strain is at the bottom of the asphalt-surfacing layer (Ullidtz 1987). Most pavement design models are therefore based on straining at the bottom of the asphalt layer to predict performance with respect to fatigue cracking (COST Action 324) (European 1997). Cumulative vertical strain on the paving layer and the subgrade produce the deformation that results in rutting (Lay 1990).

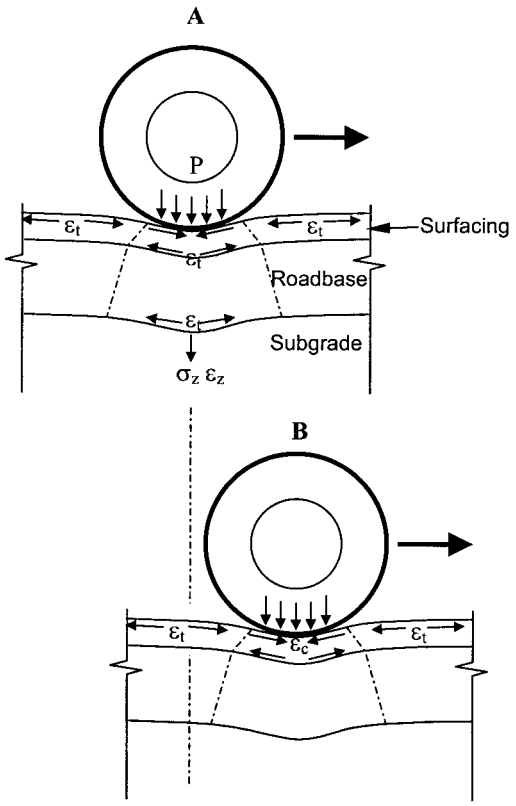

FIG. 1. Response of Flexible Pavement during Trafficking by Uniform Load *P*; Successive Wheel Positions A and B Depict Cyclic Loading That Results in Tensile ε_t and Compressive ε_c Strains in Pavement, and Compressive Stress σ_z and Strain ε_z on Subgrade

Pavement failure is determined by criteria based on longitudinal rutting or fatigue cracking in the wheel tracks. However, large elastic deflections on thin pavements with weak foundations cause fatigue failure (cracking) that undermine the substructure before appreciable rutting has occurred; hence, fatigue cracking is the limiting criterion. Structural performance of a flexible pavement based on a soft soil substratum such as peat is therefore primarily affected by factors that influence the critical tensile strain at the bottom of the surfacing layer. For any given pavement attributes, the axle load, axle configuration, suspension type, and tire inflation pressure will all affect the magnitude and distribution of stresses, strains, and displacements in its structure.

Pavement response to VTP is superficial on the paved road structure (Kim et al. 1989; Sebaaly 1992; Douglas 1999). The failure criterion for fatigue cracking of the asphalt surfacing may be evaluated from the relationship (Finn et al. 1986)

$$\log(N_f) = 16.664 - 3.291 \log\left(\frac{\varepsilon_t}{10^{-6}}\right) - 0.854 \log(E) \quad (1)$$

where N_f = number of load applications to induce fatigue cracking over 10% of the wheel path area; ε_t = horizontal

tensile strain repeatedly applied at the bottom of the asphalt concrete layer; and E = stiffness modulus for the asphalt layer (MPa).

Deterministic models (based on the elastic layer theory) using material properties and loading conditions to evaluate the strains at specified points in the pavement strata (Mahoney et al. 1994) and in-situ strain transducers (Sebaaly 1992) have been used with this relationship to quantify the efficacy of VTP for moderating pavement distress.

EXPERIMENT DETAILS

Preparation of Experimental Road Section

The experimental road section for this project was located in County Wicklow in Ireland. Initially, falling weight deflectometer readings were taken along the road in order to identify a section with uniform subgrade for location of the various measurement sensors. The identified section was excavated to 600 mm depth to the top of the subgrade over a length of 3 m. Care was taken to segregate the base and subbase materials, which were used to reconstitute the pavement after installation of the sensors.

Four pressure cells with a diameter of 229 mm (Total Earth Pressure Cell Model TP-9-S, RST Instruments Ltd., Coquitlam, British Columbia) and calibrated to 3,500 kPa were laid on top of the subgrade. Three cells were staggered under the wheel track, and a fourth was located in the center of the road as illustrated in Fig. 2. Bedding material of fine aggregates was sieved over the pressure cells to prevent large stones from pressing against the sensitive faces of the pressure cells that would cause localized pressure points. Three Campbell Scientific 257 soil moisture sensors (Campbell Scientific Inc., Leics, England) each with a reference temperature probe were inserted in the subgrade and covered with perforated plastic cups to prevent damage during compaction and to ensure proper sensor contact with the soil. The excavated area was reconstituted using the original material, by compacting a 520-mm subbase in two levels using a vibratory hand compactor. An 80-mm crushed rock base was constructed on top of the subbase to achieve the original road surface level. The instrumental area was then resealed using bitumen mix.

After 8 weeks, the areas directly above the pressure cells were smoothened using a surface grinder, and three sets of pavement strain transducers (Dynatest PAST 2-AC, Dynatest International, Duckmanton Chesterfield, U.K.) were mounted on the surface in biaxial disposition directly above the location of each pressure cell (Fig. 2). The strain transducers were rated for up to 1,500 microstrains at 110 kN/microstrain.

Fine bitumen coated aggregate was sieved over the strain transducers and then rolled manually to setting. The section was overlaid with a 50 mm (46.5 $\pm$ 4 mm) thick compacted layer of 20-mm aggregate dense base course macadam mixture [British Standard Institution (BSI) (BS 4987) 1993a]. All the transducer cables were soldered to individual sockets in a terminal box located beside the road. The section was subsequently left open to traffic over a 12-week period to enhance its conditioning, in an attempt to ensure elastic recovery or rebound deflection of its surface in the subsequent experimental loading. From the traffic counter that was installed at the site, it was estimated that 1,387 axle passes went over the experimental section during the settlement period. Core samples were taken from the extreme ends of the test section in order to determine the indirect tensile stiffness modulus (BS DD213) (BSI 1993b) of the surfacing layer (1437 $\pm$ 398 MPa).

Experimental Truck Specifications and Wheel Variables

The test section was loaded using a three axle (single tire front and dual tire rear tandem) fixed-bed timber transportation truck of 14.2 t tare weight (26 t gross vehicle weight), with a 10-spring flat-leaf suspension and fitted with 10R20 tires. The truck configuration was representative of the tractor unit in the most common tractor-trailer vehicles used by the timber industry in Ireland. The axle and wheel track spacings are shown in Fig. 2.

Four tire inflation pressure levels (350, 490, 630, and 770 kPa) were tested. The highest inflation pressure [770 kPa (110 psi)] corresponded to the normal setting (i.e., the manufacturer's recommended value for the maximum tire load rating). Truckers tend to use the manufacturer's recommended tire pressure due in part to operation safety and efficiency (Kim et al. 1989). Tire inflation or deflation was done manually using a Smat Air SA-4T150 inflation system (Explorer Engineering Corp., Oshkosh, Wis.) with a portable power source and an air compressor with a maximum working pressure of 1,050 kPa (150 psi). The system can inflate or deflate up to four tires simultaneously.

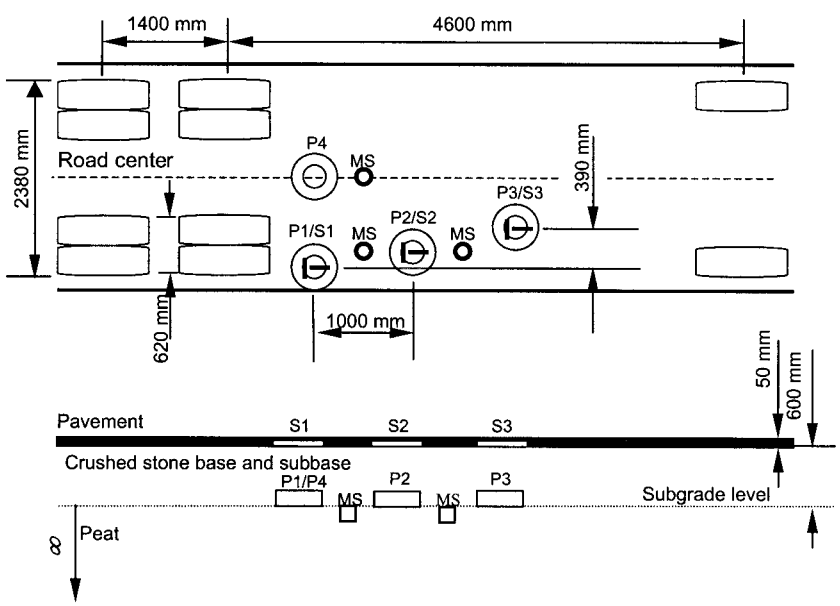

FIG. 2. Schematic of Experimental Road Section Showing Plan and Profile Location of Strain Transducers (S1, S2, S3), Pressure Cells (P1, P2, P3, and P4), and Moisture Sensors (MS); Axle Spacing and Track Width of Experimental Truck are Superimposed

TABLE 1. Variations of Static Wheel Loads, Tire Contact Area, and Mean Contact Pressure for Experimental Truck

Tire pressure [kPa (psi)]	Wheel Load (kN)[a]			Contact Area (m^2)		Mean Contact Pressure [kPa (psi)]		
	Front	Middle	Rear	Front	Rear[b]	Front	Middle	Rear
350 (50)	28.4	21.6	22.6	0.059	0.045	484 (69)	476 (68)	498 (71)
490 (70)	28.4	21.6	22.6	0.050	0.042	571 (82)	516 (74)	539 (77)
630 (90)	28.4	21.6	22.6	0.044	0.039	648 (97)	552 (79)	578 (83)
770 (110)	28.4	21.6	22.6	0.040	0.038	715 (102)	573 (82)	599 (86)
350 (50)	31.6	34.4	35.2	0.067	0.067	474 (68)	510 (73)	522 (75)
490 (70)	31.6	34.4	35.2	0.055	0.062	578 (83)	555 (79)	568 (81)
630 (90)	31.6	34.4	35.2	0.048	0.056	661 (94)	610 (87)	624 (89)
770 (110)	31.6	34.4	35.2	0.044	0.051	720 (103)	677 (97)	693 (99)
350 (50)	31.7	44.6	44.1	0.067	0.085	475 (68)	524 (75)	518 (74)
490 (70)	31.7	44.6	44.1	0.055	0.077	580 (83)	578 (83)	572 (82)
630 (90)	31.7	44.6	44.1	0.048	0.070	663 (95)	636 (91)	629 (90)
770 (110)	31.7	44.6	44.1	0.044	0.063	722 (103)	708 (101)	699 (100)

[a]Lowest, intermediate and highest values for respective wheels correspond to the empty truck, half-laden (5.8-t payload), and fully laden (9.7-t payload) truck.

[b]Contact area for rear and middle axles are equal on the basis of load sharing coefficient of unity.

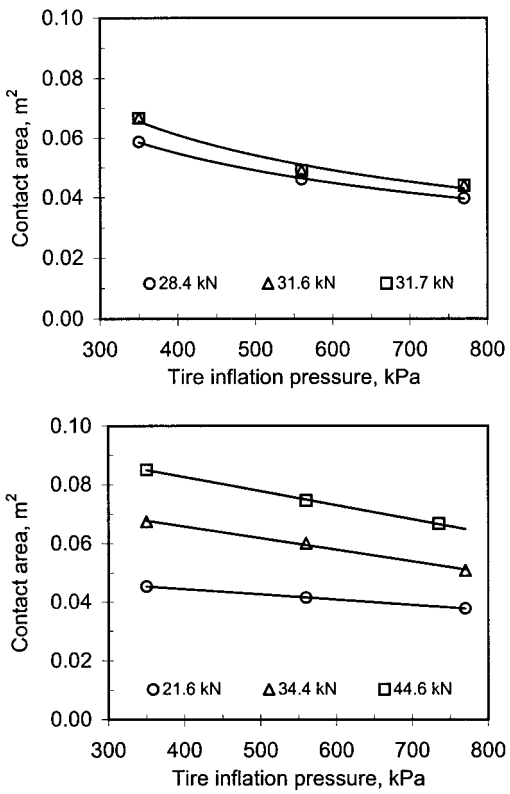

FIG. 3. Variation of Tire Contact Area with Inflation Pressure at Test Wheel Loads for Steering Wheel (Top) and Rear Dual Wheels (Bottom)

The truck was systematically loaded with timber to achieve three levels of front, middle, and rear wheel load (Table 1). The lowest values (28.4, 21.6, and 22.6 kN) and the highest values (31.7, 44.6, and 44.1 kN) for respective wheels corresponded to the empty truck and the truck stacked approximately to its capacity, respectively. The intermediate values (31.6, 34.4, and 35.2 kN) were for an approximately half-capacity truck. The load sharing coefficient (ratio of load on the heaviest axle to the average load) of the tandem axle was approximately unity, which indicates that a near perfect load distribution was achieved with this configuration.

The tire contact areas in Fig. 3 were measured on a hard concrete surface. A hydraulic jack was used to lift respective axles over a firm and smooth paper; the contact patches for the three load categories and the three tire inflation pressures (350, 570, and 770 kPa) were embossed on the paper, and the images were enhanced using black ink. The images were then scanned separately and the contact areas evaluated using the Image Tool computer program (*Image* 1997). The tire contact areas corresponding to the experimental tire pressure levels of 490 and 630 kPa for each load category (Table 1) were determined by interpolation on respective regression curves (Fig. 3), and the wheel contact pressures were then evaluated.

Data Collection Routine

The resistive bridges of the strain and pressure transducers were excited and their outputs recorded as differential voltage signals using a Campbell Scientific CR23X Micrologger (Campbell Scientific, Inc., Leics, England). A laptop computer was used for monitoring the signal inputs to the datalogger, for control of data collection, and for data retrieval.

The test section was loaded by running the truck with a preset combination of wheel load and tire inflation pressures from the same direction and reversing the truck each time for the subsequent run. Three repetitions of each combination were made with approximately 5-min intervals between the successive runs. For repeatability of the loading regime in the experimental runs, the outer steering wheel was always aligned to roll directly over a paint marker coinciding with the location of sensor group P1/S1 (Fig. 2). Consequently, the inner wheel of the middle and rear axles rolled directly over the sensor group P3/S3, while the sensor group P2/S2 measured the stress state in the intermediate area in the wheel track between P1/S1 and P3/S3. Also, a constant truck speed of approximately 0.52 m s^{-1} (2 km h^{-1}) was used in each run to control wheel-wander and to minimize the influence of road roughness. Road roughness excites the dynamic behavior in trucks, to magnify axle loads at higher speeds, and reduces the duration of load application, both of which affect the primary response of flexible pavements. The experimental road section had been resurfaced uniformly, and from visual examination the roughness was reasonably assumed to be constant.

After collection of two series of stress-strain data, the experimental section was trafficked repeatedly to failure in a separate investigation. Fatigue crack development and propagation was monitored on square grids with 300-mm sides, which were marked on the wheel track. The resulting cracks were traced on Perspex sheets at different stages of cumulative axle passes. Level readings were also taken at four cross-sectional positions across the pavement surface to monitor any progression of rut formation.

RESULTS AND DISCUSSION

The transducer outputs from the datalogger were imported into spreadsheets, and the data groups were converted to their physical quantities (stress and strain) using the multipliers and

offsets from respective transducer calibration curves. The peak strain values (longitudinal and lateral) for each wheel load and tire pressure combination were used in estimating the associated number of load repetitions to failure (fatigue life) of the asphalt surfacing layer. Vertical stress influence (VSI) which is the ratio of the normal stress on the subgrade to the tire-pavement contact pressure, was used to compare the potential of the wheels to cause rutting (Kim et al. 1989).

Characteristics of Pavement Surfacing Layer Interfacial Strains and Stress on Subgrade

Fig. 4 illustrates the typical pavement responses that were recorded in the experimental runs by the three groups of transducers (P1/S1, P2/S2, and P3/S3) in the wheel track (Fig. 2). It shows the variation of the lateral and longitudinal strains and the stress on the subgrade with successive passes of the front axle and middle and rear dual wheel axles in tandem configuration. It also shows the variation of the biaxial pavement strains and stress on the subgrade with the traverse positioning of the sensor groups.

For all the sensor groups, the longitudinal strain changes from compression (negative values) to tension (positive values) and back to compression with successive wheel passes, in a trend that is consistent with most available evidence (Huhtala et al. 1990; Siddharthan et al. 1998; Douglas 1999). The magnitude of the compressive strain prior to the tension peak was much higher than the subsequent compressive strain for the steering wheel, and it was dissipated after the rear axle (Fig. 4), which suggests that the compressive deformation in the section ahead of the loaded wheels was higher. The physical interpretation of this observation is analogous to the compressive deformation ''wave'' propagating in the direction of travel of the respective wheels. Compressive strains ahead of the steering wheel generally increased with tire inflation pressure, while those corresponding to the middle and rear dual wheels were approximately constant. Magnitudes of the compressive strain were proportional to the tensile strain with a ratio (compressive to tensile) of about 0.33 for the maximum wheel loads tested. It was also observed that the longitudinal strain dissipated rapidly with each wheel axle pass, which indicates that the pavement responded to the three axles as a series of separate and independent loads with no permanent deformation incurred. The pavement area between the middle and rear axles was mainly in compression because of their proximity to each other (1.4 m), since the section in compression ahead of individual loaded wheels extended over approximately 1 m from the center of each wheel.

With respect to sensor group P1/S1, Fig. 4 shows that the lateral strain remains tensile during the passage of each wheel load. The lateral strain under the steering wheel was higher than the corresponding longitudinal strain, but the order was reversed marginally for the dual wheels in the rear tandem axle. The asymmetric shape of the lateral strain signal and the slow rate of strain dissipation (relaxation) after passage of respective wheel loads is attributed to the viscoelastic property of the bituminous surfacing layer (Huhtala et al. 1990). The characteristic response suggests that the passage of successive axles before a complete relaxation is achieved may lead to accumulation of tension. Therefore, depending on the truck speed and axle configuration, the lateral tensile strain after the passage of successive axles could be much higher than the value corresponding to the first axle. The stress state recorded by the sensor group P1/S1 was considered to be the most important; hence, they have been used to predict pavement failure by fatigue [(1)]. Use of the fatigue model by Finn et al. (1986) in this case does not attempt to present an absolute performance of the test road pavement, but a valid in-situ pavement assessment model that would allow segregation of

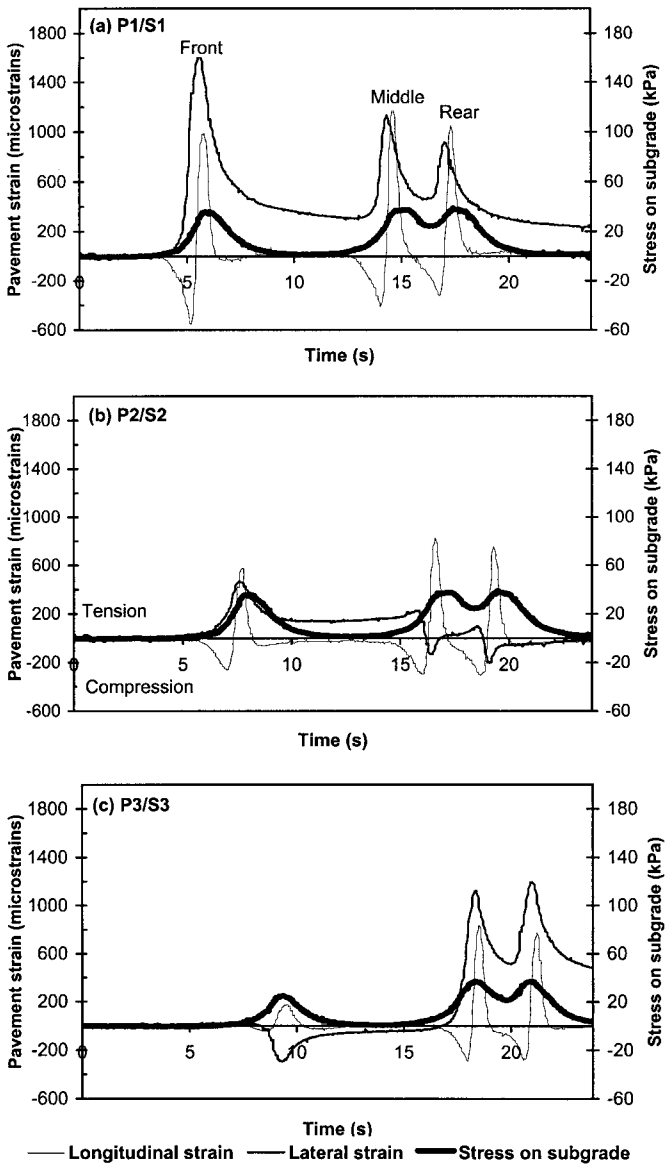

FIG. 4. Illustration of Pavement Response Output of Longitudinal and Lateral Strains, and Stress on Subgrade Corresponding to Three Transducer Groups; These Correspond to Front, Middle, and Rear Wheel Loads of 31.7, 44.6, and 44.1 kN, respectively, and Tire Inflation Pressure of 630 kPa (90 psi)

the effect of tire pressure, which was the key experimental variable.

The sensor group P3/S3 registered a compressive lateral strain with respect to the steering wheel and tensile strains for the middle and rear axles. The strain corresponding to the middle axle were comparable to those registered by the sensor group P1/S1. Those for the rear axle were higher, which suggests a disproportionate load distribution on the twin tires (Huhtala et al. 1989). The lateral strain registered by transducer group P2/S2 was tensile for the steering wheel, and compressive for the middle and rear wheels but with a tensile state in the region between these wheels. The latter observation reflects an interaction of the deformation wave from the dual wheels in the middle and rear wheels. The variation of subgrade stress under the steering wheel and pavement strain under the middle and rear dual wheels that was recorded by the three sensor groups reflects the sensitivity of the sensors to the truck position on the wheel track.

Fig. 5 shows the variation of the peak longitudinal and lateral tensile strains with tire inflation pressure under the steering wheel. The strain under the steering wheel increased uni-

formly with increasing tire inflation pressure. The experiment could not detect a difference in lateral or longitudinal tensile strains due to wheel load at the respective tire inflation pressures, which is probably due to the marginal difference in the front wheel loading for the empty truck (28.4 kN) and the fully laden truck (31.7 kN). It is also hypothesized that the increase in tire contact area due to the increased load on the single wheel counteracted the strain influence due to the axle load (Fig. 3).

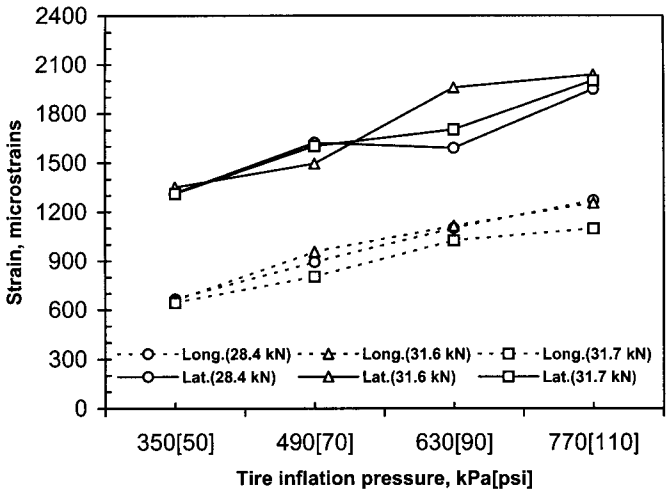

FIG. 5. Variation of Peak Longitudinal and Lateral Strains with Tire Inflation Pressure at Experimental Wheel Loads for Single Steering Wheel

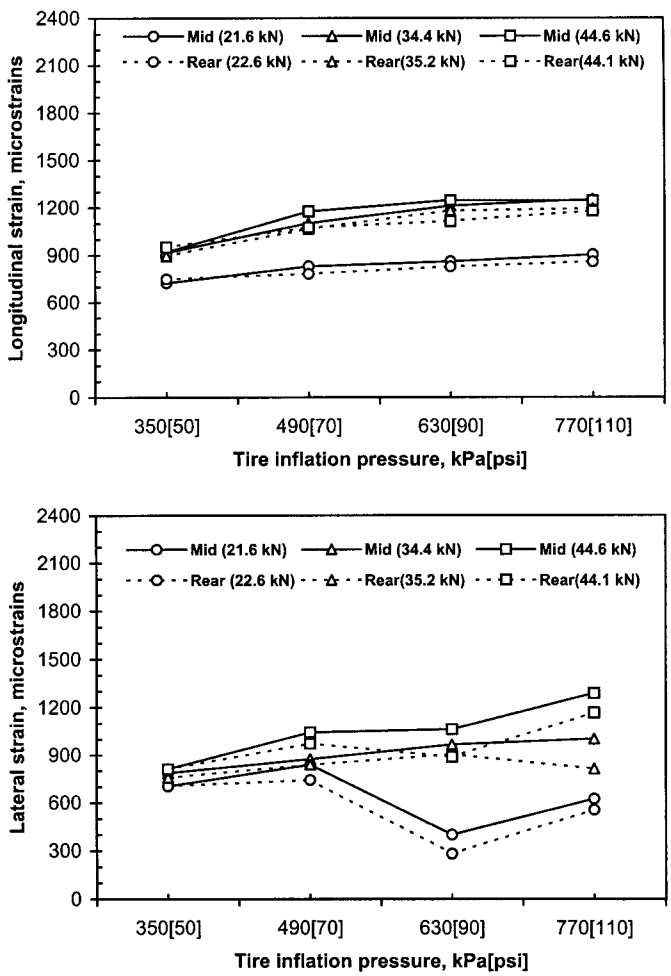

FIG. 6. Variations of Longitudinal (Top) and Lateral (Bottom) Tensile Strains with Tire Inflation Pressure at Experimental Wheel Loads for Middle and Rear Dual Wheels

Fig. 6 shows the variation of longitudinal and lateral tensile strains with tire inflation pressure with respect to the middle and rear dual wheels. It shows that the effect of tire inflation pressure was more pronounced in the range of 350–490 kPa for both the dual wheels. Also, the longitudinal tensile strains increased significantly with axle load. The mean increases corresponding to maximum wheel loads were 38 and 34% for the middle and rear dual wheels, respectively.

The lateral strains due to the steering wheel were about 77% higher than the corresponding longitudinal values, on average (Fig. 5). The difference in peak values of both longitudinal and lateral strains corresponding to the middle and rear axles reflects their load disparity (44.6 kN versus 44.1 kN). The effect of such a load disparity is magnified by the exponential relationship (Lay 1990) of the wheel load to its damage potential (peak strain in this case). It therefore underscores the importance of achieving a good load sharing with two or more axles. Fig. 6 also shows that the lateral strains due to the dual wheels (middle and rear) did not display any general trend, and analysis of the raw data indicates that they were more erratic. The evidence in Fig. 4(b) suggests the importance of the lateral positioning of the traversing dual wheel loads; hence, the observed variation in the data may have been due to experimental errors resulting from inability to precisely track the same points in each experimental run. However, it was observed that the mean values recorded were generally lower than the corresponding longitudinal values.

Stress on the subgrade also displayed peak values corresponding to the passage of individual wheel loads (Fig. 4). Peak subgrade stress under the steering wheel reduced with lateral distance from the wheel as would be expected (i.e., the stress on cell P3 was lower than P1).

Effect of Tire Inflation Pressure on Surface Distress

Figs. 7 and 8 depict the trends of the predicted [(1)] load repetitions to failure N_f or fatigue life with respect to strains under the steering wheel and the middle and rear duals, respectively. The strain values used are the peak values recorded by sensor group S1. It is shown that fatigue life N_f generally decreased with an increase in tire inflation pressure, and the magnitude of the reductions were highest in the range of 350–490 kPa. Fig. 7 suggests that the lateral strains with respect to the steering wheel would determine the initial fatigue failure of the experimental pavement, since the predicted value of N_f was lower than that with respect to longitudinal strain.

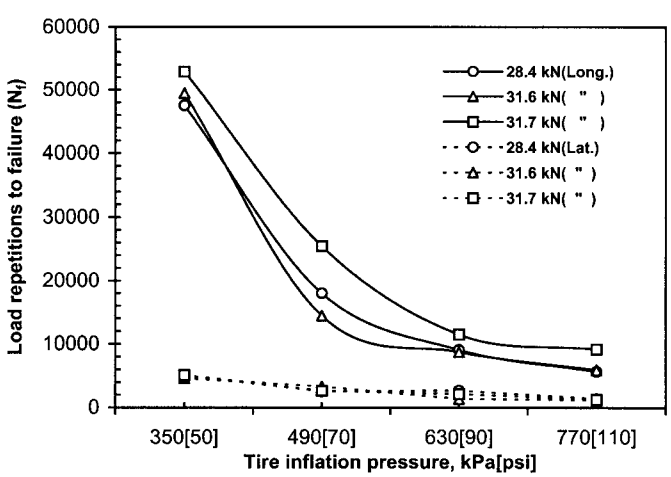

FIG. 7. Estimated Load Repetitions to Failure N_f with Respect to Longitudinal and Lateral Strains under Bound Surfacing Layer for Experimental Load Variations on Steering Wheel

Load repetitions to failure N_f with respect to the lateral strain almost doubled (93% increase) for the pressure decrease from 490 to 350 kPa. The impact of tire inflation pressure on fatigue life with respect to the longitudinal strains under the steering wheels was similar, but at less severe strain influence (higher N_f). For example, the fatigue life was about double (108% increase) with the decrease of tire inflation pressure from 490 to 350 kPa for the maximum wheel load of 31.7 kN (Fig. 7). The corresponding increases for the middle and rear dual wheels were 121% and 51%, respectively (Fig. 8). The evidence in Fig. 8 also suggests that an empty truck with high tire inflation pressure [770 kPa (110 psi)] will induce as much fatigue damage to the pavement as a fully laden truck that is operated at low [350 kPa (50 psi)] tire inflation pressures.

The increase of N_f with respect to longitudinal strains (less cracks on pavement) at lower tire pressure (Fig. 7) suggests that lower pressure may moderate the surface degradation (growth of lateral crack networks) after the initial fatigue failure caused by lateral straining. Data on surface crack propagation that were obtained, when the experimental road was trafficked to failure in the wheel tracks (Fig. 9), indicate that the predominant direction of the cracks increased from 31° to 41° to the longitudinal axis with cumulative axle passes (Hartman 2000). These corresponded to 8,898 and 13,474 axle passes of the experimental truck at the maximum load settings (Table 1). Apart from suggesting that the surfacing initially failed by predominantly longitudinal cracking, the results indicate that there was growth in lateral cracking with cumulative traffic. This evidence therefore supports the assertion that lower tire pressures will probably moderate the propagation of lateral cracks after the initial predominantly longitudinal cracking.

Fig. 10 shows the magnitude and trends of the mean of peak stress on the subgrade under the steering wheel and the middle and rear dual wheels that were recorded by pressure cell P1 (Fig. 2). With respect to the middle and rear axles, it shows that stress on the subgrade was directly proportional to the static axle load. The load variation on the steering wheel was small for the range of payload investigated, and therefore the effect of loading could not be determined with certainty. However, the data suggest a marginal increase of stress on the subgrade with tire inflation pressure.

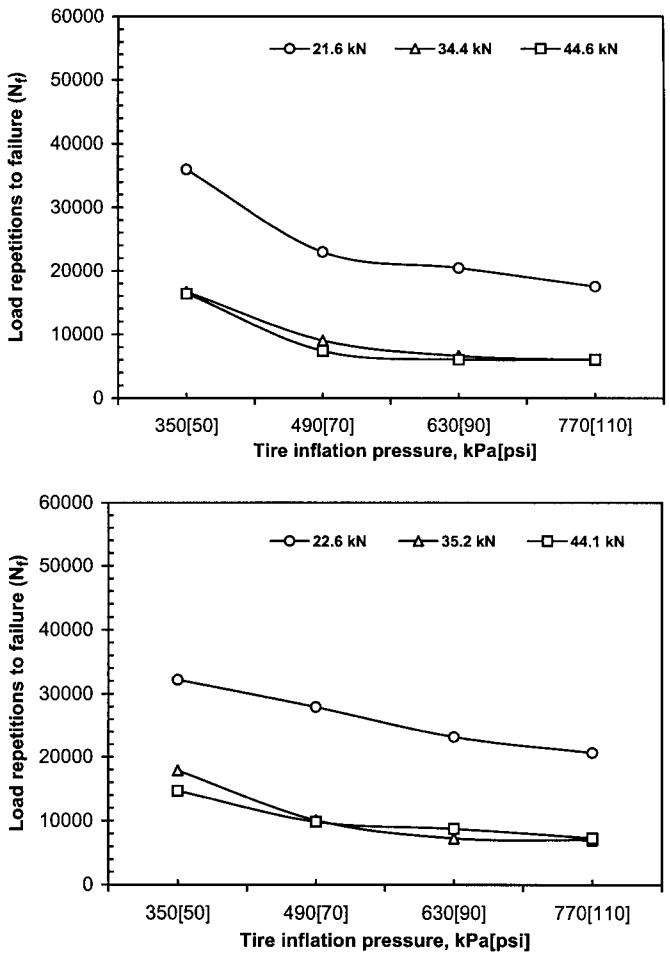

FIG. 8. Estimated Load Repetitions to Failure N_f for Varying Loads on Middle-Wheel (Top) and Rear Wheel (Bottom) with Respect to Longitudinal Strain

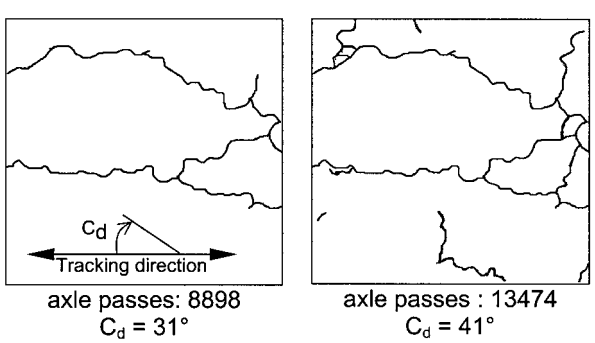

FIG. 9. Traces of Surface Crack Network Propagation on Wheel Tracks, on Square Perspex Frame with Sides of 300 mm at Two Stages of Cumulative Axle Passes (Hartman 2000); C_d Is Mean Direction of Crack Network

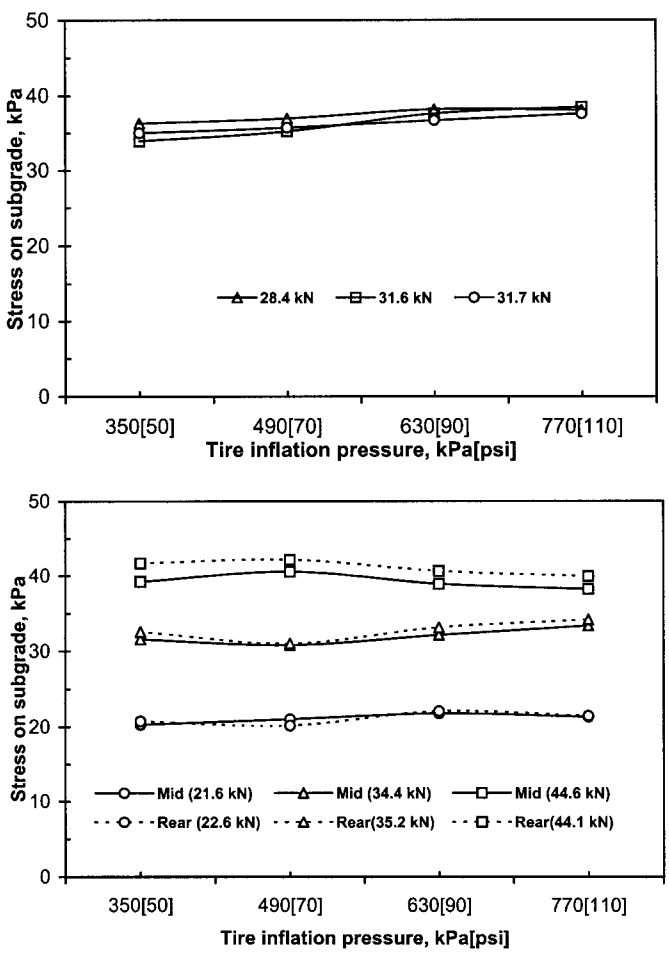

FIG. 10. Maximum Stress on Subgrade versus Tire Inflation Pressure at Respective Levels of Wheel Loads for Steering (Top) and Middle and Rear Dual Wheels (Bottom)

Effect of Wheel Load and Configuration on Surface Distress

For the middle and rear dual wheels, Fig. 8 shows that the associated fatigue life due to longitudinal strains decreased dramatically in the transition from the lowest wheel load (21.6 and 22.6 kN, respectively) to the intermediate values (34.4 and 35.2 kN, respectively). However, there was no significant difference between intermediate (34.4 and 35.2 kN) and the maximum wheel loads (44.6 and 44.1 kN). This observation suggests that pavement distress (fatigue cracks) reaches an asymptote with measured wheel load; hence, the distress may not be controlled by a reduction in axle load at economic rates of timber haulage [i.e., when the truck is loaded close to its legal load capacity (10 t/axle)]. The results in this case suggest that, to achieve a significant attenuation of the potential surface distress (fatigue cracking), the axle load should be below 50% of the axle load limit, which would be uneconomical utilization of its transportation capacity.

Compressive stress on the subgrade under the dual wheels in the tandem axle increased significantly with the wheel load for the load variation studied (Fig. 10). However, the weight transferred to the front axle due to incremental payload was observed to be relatively small. For example, for the truck payload of 10 t, the additional load on the front axle was 6.6 kN (0.67 t), which is only 6.7% of the payload. Any adverse effect of the incremental payloads is therefore in relation to the loading of the tandem axle configuration (middle and rear wheels) (i.e., truck payload had a marginal influence on the damage potential of the single steering wheel). With the maximum truck payload, the load on the single steering wheel was 31.7 kN (Table 1), while corresponding loads on the middle and rear dual wheels were 44.6 and 44.1 kN, respectively. The load ratio (rear duals to front single) was about 1.4; hence, there is insufficient evidence to evaluate the effect of wheel configuration directly. However, it is important to note that, even with such a large load disparity, the single steering wheel appeared to induce higher lateral tensile strains in the pavement; hence, the predicted lower load repetition to failure. The corresponding load ratings at maximum payload, for the single steering wheel, and the middle and rear dual wheels at the maximum tire pressures tested were 16, and 35 and 38 N/microstrain, respectively.

As with most available evidence, stress on the subgrade was mainly a function of wheel load (Fig. 10). At the maximum wheel loads investigated, stress on the subgrade due to the steering wheel (mean 36.3 kPa) was slightly lower than that due to the dual wheel in the rear tandem (means 39.2 and 41.1 kPa, respectively). VSI is defined as the ratio of the normal stress on the subgrade to the average tire-pavement contact pressure. In this study, it was found that VSI due to the steering wheel (0.06) was comparable with VSI due to dual wheels on the rear tandem (0.06 for middle wheels and 0.07 for rear wheels), at the maximum respective wheel loads. Considering that the mean contact pressure for the three wheels matched closely (Table 1), this observation suggests that the steering wheel and rear dual wheels of the experimental truck had similar potential to cause rutting.

Significance to Timber Haulage on Roads with Peat Substratum

The use of VTP systems such as CTI to balance the high inflation pressure demand of higher speeds on good quality roads, and lower pressure with slow speeds for moderation of distress on peat based roads, may enhance their serviceability. In this case, for loads up to 10 t/axle (axle load limit in Ireland) on dual wheel configuration, reducing the tire inflation pressure in the range of 770–350 kPa increased the potential pavement fatigue life by about 200%. The corresponding fatigue life with respect to the peak loading characteristics of the single steering wheel increased by 300%, with a potential for lower rate of pavement surface degradation after the initial failure. The evidence that an empty truck with high tire inflation pressure (770 kPa) will induce as much fatigue damage to the pavement as a fully laden truck that is operated at low (350 kPa) tire inflation pressures (Fig. 8) underscores the importance of appropriate truck tire pressures. However, there is need to quantify the impact of such VTP systems on truck tires, specifically, to determine the acceptable operational limits under low pressure, which may aid in optimization of the tire load ratings.

The slow dissipation of the tensile strain (Fig. 4), which was attributed to the viscoelastic nature of bituminous surfacing, has an implication for the mitigation of pavement distress with respect to speed and truck axle configuration (number and spacing). Gillespie and Karamihas (1994) reported that at low levels of road roughness, the increasing magnitude of dynamic wheel loads with speed is offset by its diminishing application time, such that damage of flexible pavements remain constant with speed. At high levels of roughness, they predicted an increase in damage with increasing speed; hence, maintenance of low road surface roughness is important. The results from this study also suggest that there may be an optimal truck axle configuration that could control the cumulative lateral strains, to minimize pavement distress; hence, there is need for further investigation in this regard.

Experimental data indicate that, for timber haulage on flexible pavements based on peat, a reduction of truck axle load primarily reduce the potential of pavement rutting. However, fatigue cracking is more critical, but reduced axle loading may not mitigate the distress potential at economic payloads. The higher potential distress due to the single steering wheel underscores a need for a more ''pavement friendly'' steering wheel specification, aimed at minimizing the surface crack distress. This requires further investigation to identify the most practical options in the wide base or alternative tire specifications (e.g., the use of optimal tread sizes, larger tires, or dual wheels).

CONCLUSIONS

From the results obtained in this project, conclusions that may be drawn are as follows for the described truck configuration:

- Lateral strain due to the steering wheel is the primary factor limiting the fatigue life of the surfacing layer of flexible pavements laid on soft soil foundations such as peat.
- While lateral pavement strain under the steering wheel control the initiation of fatigue cracking of the surfacing layer, the longitudinal strain is expected to influence the subsequent surface degradation (i.e., the extension of crack networks). The longitudinal strains increased significantly with tire inflation pressure; hence, all wheels should be operated at the lowest practicable inflation pressures.
- The slow relaxation of the tensile strain due to the viscoelastic nature of bituminous surfacing has an implication to minimizing pavement distress. It suggests that there could be a critical speed range or an optimal truck axle configuration (number and spacing) for the current load limits for road haulage; hence, there is need for further investigation in this area.
- Stress on the subgrade is mainly dependent on the axle load, which therefore determines the distress due to surface rutting. However, for roads on soft soil foundations

such as peat, fatigue cracking is critical, but reduced axle loading may not mitigate the distress potential with economic payloads.
- Lower tire pressures may enhance the serviceability of thin flexible pavements laid on subgrades of soft soil such as peat. Consequently, VTP is an option for minimizing the damage that is attributed to timber haulage trucks. Trucks fitted with CTI systems may therefore be recommended.
- There is evidence to indicate that an empty truck with high tire inflation pressure [770 kPa (110 psi)] will induce as much fatigue damage to the pavement as a fully laden truck that is operated at low [350 kPa (50 psi)] tire inflation pressures.

These may also apply to thin flexible pavements laid on soft soils other than peat.

ACKNOWLEDGMENTS

The writers would like to express their gratitude to the National Council for Forestry Research and Development (COFORD Project 3-7-1995), the Irish Forestry Board (Coillte), and Enterprise Ireland for supporting this project. Gratitude is also due to Roadstone, the National Roads Authority, and Wicklow County Council for the assistance in preparation of the experimental road section.

REFERENCES

Bradley, A. (1993). ''Testing a central tire inflation system in western Canada log-haul conditions.'' *Tech. Note TN-197: Roads and transportation*, Forest Engineering Research Institute of Canada (FERIC), Vancouver.

Bradley, A. (1996). ''Trial of a CTI system on thawing forest roads.'' *Tech. Rep. No. TR-116*, Forest Engineering Research Institute of Canada (FERIC), Vancouver.

Bradley, A. (1997). ''A literature review on the effect of variable tire pressures on roads: Summary field note.'' *Field note loading and trucking-54*, Forest Engineering Research Institute of Canada (FERIC), Vancouver.

British Standards Institution (BSI). (1993a). ''Part 1: Coated macadams for roads and other paved areas.'' *BS 4987*, London.

British Standards Institution (BSI). (1993b). ''Method for the determination of indirect tensile stiffness modulus of bituminous mixtures.'' *BS DD213*, London.

Burt, E. C., and Bailey, A. C. (1982). ''Load and inflation pressure effects on tires.'' *Trans. ASAE*, 25(4), 881–884.

De Beer, M., Fisher, C., and Jooste, F. J. (1997). ''Determination of pneumatic tire/pavement interface stresses under moving loads and some effects on pavements with thin asphalt surfacing layers.'' *Proc., 8th Int. Conf. on Asphalt Pavements*, Vol. 1, 179–227.

Douglas, R. A. (1999). ''CIT Effects in subgrades and rolling resistance.'' *Proc., Conf. on Forest Engrg. for Tomorrow: Machinery*, Paper No. 4, Forest Engrg. Group, U.K. Institution of Agricultural Engineer, Silsoe, U.K.

Dunlop Tire Corporation. (1998). *Tire care and maintenance: Inflation*, Buffalo.

European Commission. (1997). ''Long term performance of road pavements.'' *Cost Action, 324 Final Rep.*, Office for Official Publication of the European Communities, Luxembourg.

Finn, F., Saraf, C. L., Kulkarni, R., Nair, K., Smith, W., and Abdullah, A. (1986). ''Development of pavement structural subsystems.'' *NCHRP Rep. 291*, Transportation Research Board, Washington, D.C.

Foltz, R. B. (1994). ''Reducing tire pressure reduces sediment.'' *Tech. Tips, July 1994*: *Roads*/*Timber*, USDA Forest Services SDTDC, San Dimas, Calif.

Foltz, R. B., and Elliot, W. J. (1997). ''The impact of lowered tire pressures on road erosion.'' *76th Annu. Meeting of the Transp. Res. Board (TRB)*. Transportation Research Board, Washington, D.C.

Gillespie, T. D., and Karamihas, S. M. (1994). ''Heavy truck properties significant to pavement damage.'' *Vehicle-road interaction, ASTM STP 1225*, ASTM, West Conshohocken, Pa., 52–63.

Grau, R. W. (1993). ''Effects of variable tire pressure on road surfacings.'' *Design, construction, behaviour under traffic, and test results*, Vol. 1, *Tech. Rep. GL-93-20*, U.S. Army Engineer Waterways Experiment Station, Vicksburg, Miss.

Hartman, A. M. (2000). ''An experimental investigation into the mechanical performance and structural integrity of bituminous road pavement mixtures under the action of fatigue load conditions.'' PhD thesis. Dept. of Mech. Engrg., University College Dublin, Dublin, Ireland.

Huhtala, M., Alkio, R., Pihljamaki, J., Pienimaki, M., and Halonan, P. (1990). ''Behaviour of bituminous materials under moving wheel loads.'' *Proc., Assn. of Asphalt Paving Technologists*, 59, 422–442.

Huhtala, M., Pihljamaki, J., and Pienimaki, M. (1989). ''Effect of tires and tire pressures on road pavements.'' *Transp. Res. Rec. 1227*, Transportation Research Board, Washington, D.C., 107–114.

Image tool version 1.27. (1997). ⟨http://macorb.uthscsa.edu/dig/itdesc.html⟩. University of Texas Health Science Center at San Antonio, San Antonio.

Irish Forestry Board (Coillte). (1991). ''Development of a timber allocation procedure.'' Dublin.

Irish Forestry Board (Coillte). (1998). ''A framework for sustainable forest management.'' Dublin.

Jakobsen, B. F., and Dexter, A. R. (1989). ''Prediction of soil compaction under pneumatic tires.'' *J. Terramech*., Elsevier, Oxford, U.K., 26(2), 107–119.

Kestler, M., Berg, R. L., and Moore, T. L. (1997). ''Using reduced tire pressure to reduce damage to low-volume roads.'' *76th Annu. Meeting of the Transp. Res. Board (TRB)*, Transportation Research Board, Washington, D.C.

Kim, O., Bell, C. A., and Wilson, J. E. (1989). ''Effect of increased truck tire pressure on asphalt concrete pavements.'' *J. Trans. Engrg*., ASCE, 115(4), 329–350.

Lay, M. G. (1990). *Handbook of road technology, Volume 1: Planning and pavements*, Gordon and Breach, New York, 277–292.

Mahoney, J. P., Sweet, B. R., Copstead, R. W., and Keller, R. R. (1994). ''The potential use of CTI during highway load restriction periods.'' *SAE Tech. Paper No. 942245*.

Moore, T. L. (1997). ''Implementation of variable tire pressure technology in the USDA Forest Service.'' *76th Annu. Meeting of the Transp. Res. Board (TRB)*, Transportation Research Board, Washington, D.C.

National Council for Forest Research and Development (COFORD). (1994). ''Pathway to progress: A programme for research and development: harvesting and transport.'' Ireland, 57–75.

O'Mahony, M. J., Ueberschaer, A., Owende, P. M. O., and Ward, S. M. (2000). ''Bearing capacity of forest access roads built on peat soils.'' *J. Terramech*., Elsevier, Oxford, U.K., 37(3), 127–138.

Raper, R. L., Bailey, A. C., Burt, E. C., Way, T. R., and Liberati, P. (1995). ''The effects of reduced inflation pressure on soil-tire interface stresses and soil strength.'' *J. Terramech*., Elsevier, Oxford, U.K., 32(1), 43–51.

Schwanghart, H. (1991). ''Measurement of contact area, contact pressure and compaction under tires in soft soil.'' *J. Terramech*., Elsevier, Oxford, U.K., 28(4), 309–318.

Sebaaly, P. E. (1992). ''Pavement damage as related to tires, pressures, axle loads, and configurations.'' *Vehicle, tire, pavement interface, ASTM STP 1164*, ASTM, West Conshohocken, Pa., 54–68.

Siddharthan, R. J., Yao, J., and Sebaaly, P. E. (1998). ''Pavement strain from moving dynamic 3D load distribution.'' *J. Transp. Engrg*., ASCE, 124(6), 557–566.

Tire Pressure Control International Ltd., (1998). *Redline-Eltek tire pressure control systems*, Edmonton, Canada.

Ullidtz, P. (1987). *Pavement analysis*, Elsevier, Amsterdam, 177–198.